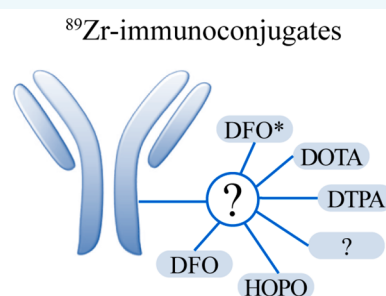# 89Zr-Immuno-Positron Emission Tomography in Oncology: State-of-the-Art 89Zr Radiochemistry

Sandra Heskamp,[†] René Raavé,[†] Otto Boerman,[†] Mark Rijpkema,[†] Victor Goncalves,[‡] and Franck Denat*,[‡]

[†]Department of Radiology and Nuclear Medicine, Radboud University Medical Center, Geert Grooteplein-Zuid 10, 6525 HP Nijmegen, The Netherlands

[‡]Institut de Chimie Moléculaire de l'Université de Bourgogne, UMR6302, CNRS, Université Bourgogne Franche-Comté, F-21000 Dijon, France

**ABSTRACT:** Immuno-positron emission tomography (immuno-PET) with 89Zr-labeled antibodies has shown great potential in cancer imaging. It can provide important information about the pharmacokinetics and tumor-targeting properties of monoclonal antibodies and may help in anticipating on toxicity. Furthermore, it allows accurate dose planning for individualized radioimmunotherapy and may aid in patient selection and early-response monitoring for targeted therapies. The most commonly used chelator for 89Zr is desferrioxamine (DFO). Preclinical studies have shown that DFO is not an ideal chelator because the 89Zr−DFO complex is partly unstable in vivo, which results in the release of 89Zr from the chelator and the subsequent accumulation of 89Zr in bone. This bone accumulation interferes with accurate interpretation and quantification of bone uptake on PET images. Therefore, there is a need for novel chelators that allow more stable complexation of 89Zr. In this Review, we will describe the most recent developments in 89Zr radiochemistry, including novel chelators and site-specific conjugation methods.

## ROLE OF 89ZR-IMMUNOPET IN DRUG DEVELOPMENT AND PERSONALIZED CANCER TREATMENT

In past years, immuno-positron emission tomography (immunoPET) with 89Zr-labeled antibodies (89Zr-immunoPET) has shown great potential in cancer imaging. It can play an important role in early drug development and molecular characterization of tumors for individualized anticancer treatment. 89Zr-immunoPET provides important information about the pharmacokinetics and tumor (and normal tissue) targeting properties of monoclonal antibodies.[1−3] A safety issue in drug development is the maldistribution of large-molecule drugs, resulting in an adverse balance between safety (from effects in nontarget tissues) and efficacy (on-target effects in target tissues). 89Zr-immunoPET imaging could help in two ways: (1) in animal models to avoid selection of molecules with a propensity for maldistribution and (2) in clinical development to reduce incidence of maldistribution in trial subjects exposed to the investigational new macromolecular drug. 89Zr-immunoPET is also an important tool to noninvasively assess the expression and accessibility of target antigens in tumors and normal tissues for patient selection and early-response monitoring of targeted therapies.[4−6] In this regard, 89Zr-immunoPET has several advantages over conventional approaches such as tumor biopsies and immunohistochemistry. First of all, it allows the measurement of target expression of

whole tumor lesions and their metastases, thereby avoiding misinterpretation due to tumor heterogeneity or sampling error. Furthermore, it allows the longitudinal monitoring of target expression, which could be of clinical relevance because target expression can change in time during disease progression or treatment. Finally, in vivo imaging also takes into account target accessibility after systemic administration. Next to target expression, factors such as vascular permeability, interstitial fluid pressure, blood flow, and vessel density affect the uptake of a monoclonal antibodies in a tumor. If target accessibility is low, the therapeutic agent might not reach the tumor cells despite adequate expression of the target.[7−9] A final application of 89Zr-immunoPET is accurate dose planning for individualized radioimmunotherapy with 177Lu- or 90Y-labeled antibodies, such as, for example, for 90Y-ibritumomab tiuxetan therapy.[10,11]

## ADVANTAGES AND LIMITATIONS OF 89ZR-IMMUNOPET

For imaging purposes, immunoPET is preferred over immunoSPECT because of the higher resolution, sensitivity, and more-accurate image quantification. 89Zr is an ideal

radionuclide for immunoPET. It decays via positron emission and electron capture to $^{89m}$Y, which in turn decays via $\gamma$ ray emission (909 keV) to stable $^{89}$Y. The 78.4 h half-life of $^{89}$Zr perfectly matches with the pharmacokinetics of monoclonal antibodies that typically show optimal tumor-to-blood ratios several days after injection. The relatively low-energy positrons ($E_{mean}$ 395 keV) provide high-resolution PET images. Importantly, $^{89}$Zr is a residualizing radionuclide: upon internalization, it is trapped inside the tumor cell, which results in improved tumor retention and enhanced tumor-to-normal tissue ratios, as compared with nonresidualizing radionuclides such as iodine-124 ($^{124}$I).[12]

Although $^{89}$Zr-immunoPET is a highly attractive technique to measure tumor-associated antigens and to measure the in vivo distribution of monoclonal antibodies, but it also has a few limitations. First of all, the enhanced permeability and retention effect may result in non-receptor-mediated uptake of radio-labeled antibodies leading to false-positive results. Second, low target expression may lead to false-negative results due to low imaging contrast because of the long circulatory half-life of monoclonal antibodies. Third, $^{89}$Zr has a low positron abundance of only 23%, compared with those of $^{18}$F (97%) and $^{68}$Ga (89%) but similar to that of $^{124}$I (23%). Finally, for each $^{89}$Zr-immunoPET scan, patients are exposed to relatively high doses of radioactivity, which limits the possibility for longitudinal studies, especially for patients who are treated with curative intent.

## $^{89}$ZR-IMMUNOPET IN PRECLINICAL AND CLINICAL STUDIES

Meijs et al. were the first to show the potential of $^{89}$Zr-labeled antibodies for PET imaging. The $^{89}$Zr-labeled anti-EpCam antibody 323/A3 was successfully used to visualize human OVCAR-3 xenografts in immunodeficient mice.[13] Since then, numerous $^{89}$Zr-labeled antibodies have been developed targeting several tumor-associated antigens, i.e. EGFR, HER2, CD44v6, PSMA, CD20, and VEGF-A.[14,15] During the past years, $^{89}$Zr-immunoPET has been successfully translated to cancer patient populations in various studies.[14]

The first clinical $^{89}$Zr-immunoPET study was reported by Börjesson et al. They showed that primary squamous cell carcinomas (HNSCC) could be detected by PET imaging using $^{89}$Zr-labeled chimeric anti-CD44v6 antibody U36.[1] Since then, several studies have successfully used $^{89}$Zr-immunoPET for tumor imaging. One prime example is immunoPET with $^{89}$Zr-trastuzumab. Dijkers et al. have shown that $^{89}$Zr-trastuzumab immunoPET can detect metastatic liver, lung, bone, and even brain lesions in patients with HER2-positive breast cancer (Figure 1).[2] Furthermore, $^{89}$Zr-trastuzumab immunoPET was able to solve a clinical dilemma in a patient with suspected liver and mediastinal metastases, which could not be confirmed by biopsies.[5] Finally, $^{89}$Zr-trastuzumab immunoPET has been used to predict and monitor therapy response.[6,16] It must be noted that for many lesions, HER2 expression was never demonstrated, so future studies should confirm the correlation between $^{89}$Zr-trastuzumab uptake and HER2 expression levels. An overview of (pre)clinical $^{89}$Zr-immunoPET studies has been described in detail in several excellent reviews.[14,15,17,18]
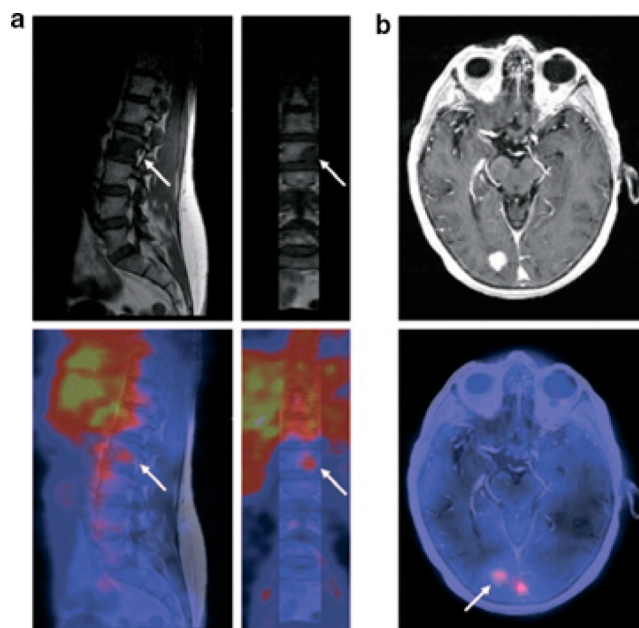


**Figure 1.** Example of fusion images from $^{89}$Zr–trastuzumab HER2 PET and MRI scans of a (a) vertebral metastasis and (b) brain metastases. Reprinted with permission from ref 2. Copyright 2010 Wiley.

## CURRENT CHALLENGES IN $^{89}$ZR RADIOCHEMISTRY

Although preclinical and clinical studies clearly indicate the potential of $^{89}$Zr-immunoPET for cancer imaging, from a chemical point of view, the current radiotracers are suboptimal. An ideal $^{89}$Zr-labeled antibody for immunoPET should fulfill the following criteria:

1) safe for clinical use;
2) unchanged pharmacokinetics compared to the unconjugated antibody;
3) unchanged affinity for its target; and
4) no release of $^{89}$Zr.

Currently, the most commonly used chelator for $^{89}$Zr is desferrioxamine (DFO). Preclinical studies have shown that DFO is a not an ideal chelator because the $^{89}$Zr–DFO complex is partly unstable. This results in release of $^{89}$Zr from the chelator and the subsequent accumulation of $^{89}$Zr in bone tissue that can reach values >10% ID/g.[10,19−22] It has been suggested that $^{89}$Zr bone uptake can be attributed to a metabolic process, as it seems to be more-pronounced for internalizing antibodies compared with noninternalizing antibodies. After the internalization and catabolization of the $^{89}$Zr–DFO–antibody conjugate in the lysosomes, the $^{89}$Zr may be released from the chelator and subsequently leave the cell.[10,19,20,22]

Several studies have shown a mismatch between the $^{89}$Zr-labeled antibody and $^{111}$In- or $^{177}$Lu-labeled antibody with respect to bone uptake. The bone uptake of released $^{89}$Zr is undesired because it may hamper the detection of bone metastases. Furthermore, it will overestimate the tracer uptake in bone tissues and could lead to overestimation of the radiation dose to the bone marrow in case of dose planning for radioimmunotherapy. Therefore, there is a need for novel chelators that allow more stable complexation of $^{89}$Zr. The importance of the choice of the bifunctional chelating agent in
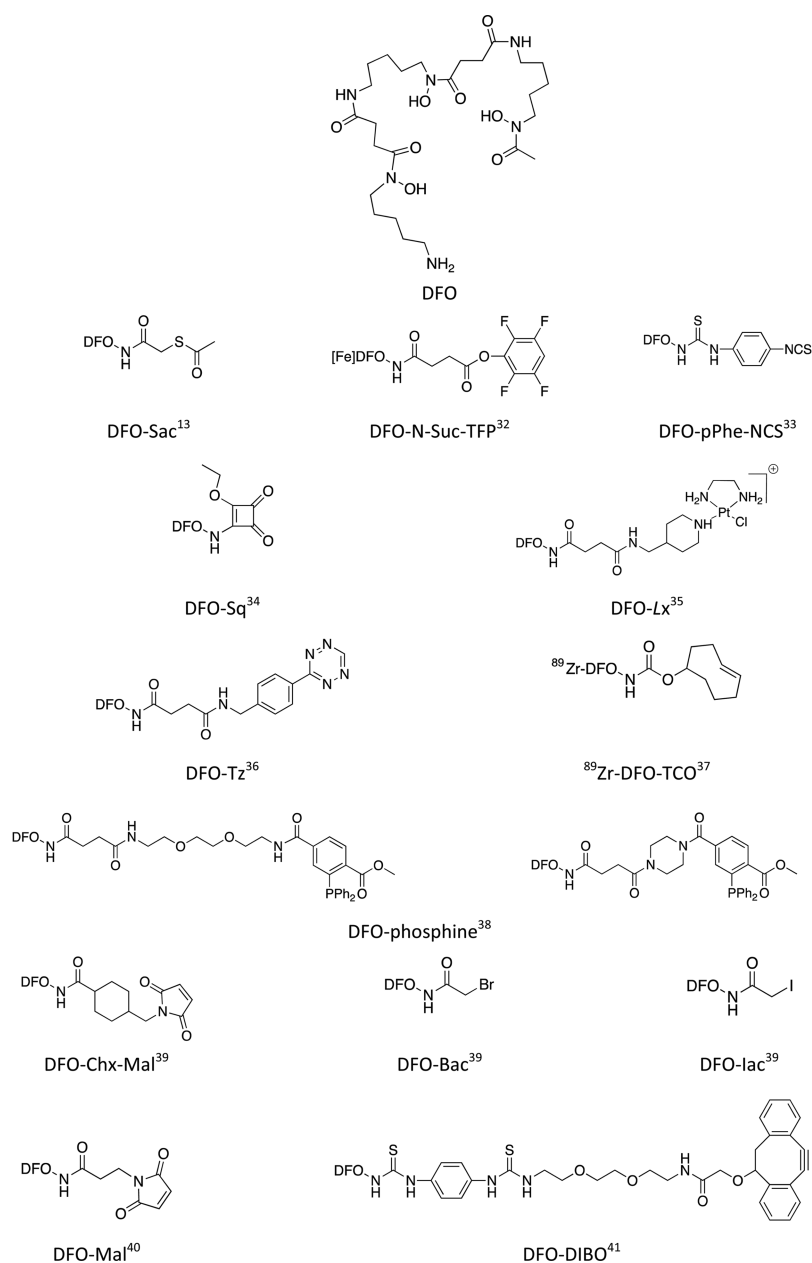
**Figure 2.** DFO and its bifunctional versions.

the design of a metal based radiopharmaceutical has been demonstrated in a large number of studies and highlighted in several reviews in the past few years.[23−26]

Another challenge in $^{89}$Zr-immunoPET is the antibody-chelator conjugation without affecting immunoreactivity and binding affinity. Conjugation of antibodies with bifunctional chelators is mostly based on random reactions with the $\varepsilon$-amino group of lysine residues. However, if the antigen binding domain of the antibody contains critical lysines residues, the chelator may alter the antigen binding affinity and reduce the immunoreactivity of the antibody. These challenges may be overcome by site-specific conjugation techniques. These techniques result in chemically defined antibody-chelator conjugates, while random conjugation results in mixtures of antibody-chelator conjugates with different substitution ratios. Several site-specific conjugation strategies have been developed.[27,28] In this Review, we will describe the most recent developments in $^{89}$Zr-radiochemistry, including site-specific

conjugation methods and novel chelators (for previous reviews on $^{89}$Zr radiochemistry, see refs 15, 29, and 30). We will focus on antibody-based radiotracers; however, the described developments are also hihgly relevant for other types of radiotracers, including antibody fragments, nanobodies, affibody molecules, and peptides.

## $^{89}$ZR BIFUNCTIONAL CHELATING AGENTS: THE CURRENT STATE OF THE ART

**DFO and DFO-Based Bifunctional Chelators.** DFO, also called deferoxamine, desferrioxamine B, desferoxamine B, MPO-B, DFOA, DFB, or Desferal (Figure 2), is by far the most commonly used chelator for $^{89}$Zr-immunoPET. It was found 25 years ago that this natural bacterial siderophore binds $^{89}$Zr much more efficiently than diethylenetriaminepentaacetic acid (DTPA).[31] Different approaches have been proposed for

the conjugation of DFO to antibodies, involving various bifunctional versions of DFO (Figure 2).[15,30]

*Random Bioconjugation of DFO-Based Bifunctional Chelators.* The most-common approach is the random conjugation to lysine residues of antibodies. Meijs et al. used a two-step procedure to introduce DFO into two different mAbs (E48 and 323/A3).[13] In the first step, maleimide groups were incorporated into the mAbs through the reaction of lysines with 4-(*N*-maleimidomethyl) cyclohexane carboxylic acid *N*-hydroxysuccinimide ester (SMCC). DFO was converted to its *S*-acetyl protected thiol derivative (DFO-Sac) by reaction with *N*-succinimidyl-*S*-acetylthioacetate (SATA). The two products were reacted with each other in the presence of hydroxylamine, and the resulting bioconjugates were purified by gel filtration to remove the excess of DFO–Sac. The bioconjugates were labeled with $^{89}$Zr with a specific activity of 5 mCi/mg. Biodistribution studies in tumor bearing mice showed a high tumor uptake of the conjugates but also a high background accumulation of $^{89}$Zr in other tissues. This might be due to the cleavage of the succinimide–thioether bond, which results in the release of the chelator from the antibody.

Most of the in vivo studies reported so far involved antibodies modified with DFO bearing either an activated ester (DFO−*N*-Suc−TFP) or an isothiocyanate function (DFO−pPhe−NCS).[32,42]} The activated ester strategy, developed by Verel et al., involves six successive steps: (i) DFO was succinylated; (ii) the modified DFO was metalated with $Fe^{3+}$; (iii) it was reacted with tetrafluorophenol to give the activated ester DFO−*N*-Suc−TFP, which was (iv) conjugated to the antibody (an anti-CD44v6 chimeric mAb U36 directed against head and neck cancer in the pioneer work of Verel et al.) with a chelator-to-mAb ratio of about 1:1; and (v) the product was demetalated by transchelation with excess EDTA and (vi) radiolabeled with $^{89}$Zr. The protection of DFO by $Fe^{3+}$ complexation is mandatory to prevent side-reactions during the formation of the activated tetrafluorophenolic ester. The method is synthetically demanding, but the [Fe]DFO−*N*-Suc−TFP can be stored for at least one year and is commercially available. Also, it has to be mentioned that the removal of iron after conjugation requires low pH (between 4.2 and 4.5), which can have deleterious effects on some proteins. However, this strategy yields $^{89}$Zr-labeled antibodies with favorable in vitro and in vivo behaviors, and it has been used for labeling a wide range of mAbs. Another efficient route for incorporating DFO into biologicals, developed more recently by the same research group from Amsterdam, is the use of a *p*-isothiocyanatophenyl derivative DFO−pPhe−NCS.[33,42] They reported on the conjugation of this bifunctional chelating agent to three mAbs (U36, cetuximab, and rituximab) with a 1.5:1 chelator-to-mAb ratio, regardless of the nature of the antibody. Upon storage in NaCl containing buffers, the immunoconjugates appeared to be less stable than the analogs obtained through the DFO−*N*-Suc−TFP route, probably due to the reaction of thiourea bond with hypochlorite ions formed upon radiation. However, in vivo studies revealed comparable behavior of the conjugates prepared by the two methods and this more straightforward route has become a standard protocol for $^{89}$Zr-DFO labeling of antibodies. It has to be noted that the poor water solubility of DFO−pPhe−NCS requires the use of a small amount of DMSO, and precautions have to be taken during the conjugation step to prevent protein degradation. Donnelly and co-workers proposed an alternative to DFO−pPhe−NCS by attaching a squaramide ester to DFO.[34] Because

this new bifunctional DFO derivative, DFO−Sq can be considered an extended DFO; this work will be discussed in the Hydroxamate-Based Chelators (DFO Analogs) section.

Very recently, Sijbrandi et al. developed a new $^{89}$Zr−DFO trastuzumab conjugate using a novel linker technology called *Lx*.[35] *Lx* stands for a metal−organic linker based on ethylenediamineplatinum(II). The platinum complex was first coordinated to a DFO derivative to give a stable and storable compound, with increased water solubility, which was then conjugated to trastuzumab to yield the immunoPET conjugate. The DFO-to-mAb ratio in this conjugate was determined to be 2.6. Interestingly, the characterization of fragments obtained by papain or pepsin digestion shown that 85% of the payload was bound to the Fc region of the mAb, which reduces the chance of affecting the immunoreactivity. It was also shown that the platinum derivative was more likely coordinated to histidine residues, thus offering a valuable alternative to the conventional coupling to lysine or cysteine residues. The conjugates were stable in vivo, a comparative biodistribution study of $^{89}$Zr−DFO−*Lx*−trastuzumab and $^{89}$Zr−DFO−trastuzumab prepared by the DFO−*N*−Suc-TFP route showed similar $^{89}$Zr uptake in the tumor and all organs with the exception of the liver (5.4 ± 0.8 and 4.0 ± 0.3%ID/g for $^{89}$Zr−DFO−*Lx*−trastuzumab and $^{89}$Zr−DFO−trastuzumab, respectively).

The use of click chemistry has emerged as an alternative method for the design of radiolabeled compounds for both imaging and therapeutic purposes.[43] The click chemistry tool box has been incredibly expanded in the last years, providing numerous ligation methods for bioconjugation with many advantages: fast, quantitative, clean, selective, and biorthogonal, allowing site-specific approaches (see the Site-Specific Bioconjugation of DFO-Based Bifunctional Chelators section) and in vivo pretargeting.

Zeglis et al. used this approach for radiolabeling trastuzumab with either $^{89}$Zr or $^{64}$Cu.[36] They used the well-known inverse electron demand Diels−Alder reaction (IEDDA) between norbornene and tetrazine to introduce a bifunctional chelator. In the first step, the mAb was reacted with norbornene succinimidyl ester. The resulting modified antibody, which can be stored at 4 °C for a long period, was then coupled to a tetrazine-containing chelator (DFO−Tz or DOTA−Tz) to yield the final immunoconjugates ready to be metalated with $^{89}$Zr or $^{64}$Cu. The coupling reaction was performed in mild conditions but required a relatively long incubation time (5 h). The chelator-to-mAb ratio ranged from 1.1 to 3.8, depending on the amount of norbornene−NHS−ester used in the first step. Although the $^{89}$Zr-labeled conjugate was stable in human serum at 37 °C for 48 h, in vivo studies in mice showed relatively high bone uptake (up to 15.2% ID/g after 72 h). Above all, this work is a nice proof of concept of the modularity of the click-chemistry approach.

More recently, Meimetis et al. developed a similar strategy for the synthesis of a dual labeled trastuzumab for bimodal imaging (PET and fluorescence imaging).[44] In this work, transcyclooctene (TCO)−PEG$_4$−NHS was conjugated to trastuzumab, and then the resulting trastuzumab−TCO was coupled via IEDDA reaction to a bimodal probe containing both DFO, a BODIPY moiety, and a tetrazine unit. The click reaction of TCO with tetrazine was much more rapid than the one with norbornene and was completed within 3 min to yield two conjugates with different degrees of labeling (ca. 1 and 2.5 probes per antibody, these values being determined by mass spectrometry and UV−vis measurements). Surprisingly, the

bimodal immunoconjugate exhibited a 4-fold higher tumor uptake in HER2$^+$ tumors bearing mice in comparison to the conjugate prepared by the conventional DFO−N-Suc−TFP method. However, a 2.5-fold higher liver uptake was also observed, probably due to the enhanced lipophilicity introduced by the BODIPY dye. Interestingly, no significant difference between the conjugates prepared by the two different routes was observed for bone uptake, which remained relatively low (3.52% ID/g). The TCO−tetrazine click reaction has been also used in a reverse way (the TCO was appended to DFO) for labeling a peptide with $^{89}$Zr.[37]

Another click-chemistry reaction, the Staudinger ligation, was investigated for labeling chimeric mAb U36 with $^{89}$Zr−DFO in a pretargeting approach.[38] Up to 8 triazide moieties (24 azide functions) could be incorporated into the mAb without affecting significantly the immunoreactivity. A pair of $^{89}$Zr−DFO−phosphine derivatives were synthesized and their Staudinger ligation with the U36-triazide was studied. The reaction was quite slow in PBS (20−25% after 2h at 37 °C) and even slower in human serum and, unfortunately, was not observed in vivo. This study showed that Staudinger ligation is not the method of choice, at least with the aim of in vivo pretargeting.

*Site-Specific Bioconjugation of DFO-Based Bifunctional Chelators.* One major drawback of the methods described above is that the random conjugation of the probe to amino-acid residues within the antibody (e.g., lysines) leads to poorly chemically defined biologics. This lack of specificity and homogeneity, both with respect to the BFC-to-mAb ratio and the site of conjugation, may result in in vivo behavior of the conjugate that is less efficient. In particular, the attachment of the bifunctional chelator to the antigen-binding domains of the antiboby may lower its immunoreactivity. Inspired by the exponentially growing field of bioconjugation techniques for the synthesis of antibody−drug conjugates (ADC),[45,46] increasing attention has been paid in the last years to the use of site-specific labeling of antibodies also for molecular imaging.[27,28] A precise control of the number and the location of the chelators on the antibody should result in better-defined and more-efficient immunoconjugates and more easily reproducible procedures and may facilitate the approval process.

Tinianow et al. from Genentech were the first to report a site-specific conjugation route for the synthesis of $^{89}$Zr immunoconjugates using maleimide- and halide-modified DFO.[39] The authors used a bioengineered mAb, so-called thio-trastuzumab, containing two cysteine residues in the heavy chain. These unpaired cysteines incorporated into nonbioactive sites of the antibody were reacted with either bromoacetyl− or iodoacetyl−DFO (DFO−Bac and DFO−Iac) through nucleophilic substitution or with a maleimide derivative (DFO−Chx−Mal) via Michael addition. Among the three thiol-reactive DFO derivatives investigated, DFO−Chx−Mal proved to be the best candidate in terms of bioconjugation and radiolabeling efficiency. Indeed, the resulting bioconjugate containing exactly two chelators per antibody was obtained after 1 h of incubation of the BFC with thio-trastuzumab at room temperature at pH 7.5. Radiometalation with $^{89}$Zr-oxalate gave the $^{89}$Zr-labeled conjugate with the highest radiochemical yield (87.5%) and purity (98%), in comparison with the two others site-specifically prepared immunoconjugates and the two analogs prepared by conventional routes (DFO−N-Suc−TFP and DFO−pPhe−NCS). However, in the model employed in this

study, the site-specific approach did not show significant advantage over the random conjugation route.

Ma et al. also used a maleimide-modified DFO, the maleimidopropionate−DFO (DFO−Mal), which was conjugated to trastuzumab after reduction of disulfide bonds with Tris(2-carboxyethyl) phosphine (TCEP). The biodistribution of the resulting highly loaded bioconjugate (containing between four and eight chelators per antibody) in normal mice was studied with the aim to compare DFO with a new tripodal chelator (see the Hydroxypyridinone-, Terephthalamide-, and Catecholate-Based Chelators section).[40]

Schibli and co-workers used a method based on enzymatic modification of antibodies for the site-specific incorporation of DFO into two antibodies, chimeric CE7 and rituximab, targeting, respectively, L1CAM and CD20.[47] In this work, the mAbs were first enzymatically deglycosylated to differentiate selectively two glutamine residues in the Fc region, which can undergo further reaction with DFO catalyzed by bacterial transglutaminase (BTG). In a variant of this approach, they also developed a chimeric CE7 mutant in which two asparagines were replaced by glutamines, thus allowing the introduction of four chelators per antibody. In vivo distribution in tumor bearing mice revealed that engineered bioconjugates labeled with $^{67}$Ga showed higher tumor-to-liver ratio compared to those prepared by conventional routes. However, the biodistribution study with $^{89}$Zr analogs was not reported, and PET images did not evidence a superior behavior of the engineered bioconjugate.

Enzyme-mediated methodologies represent an efficient tool for site-specific introduction of cytotoxic payloads on the heavy chain glycans of mAbs[48] and also for the development of site-specifically labeled immunoconjugates.[41] In their work, Zeglis et al. used β-1,4-galactosidase to remove terminal galactose residues on the Fc domain of an antibody targeting PSMA (J591), which were then replaced by N-azido-acetylgalactos-amine (GalNAz) using a mutant β-1,4-galactosyltransferase Gal-1T1(Y289L) to afford the modified J591 bearing biorthogonal azido groups. The DFO conjugate was finally obtained by clicking on N$_3$-J591, a DFO bearing a dibenzocyclooctyne unit (DFO−DIBO), following the well-known strain promoted alkyne−azide cycloaddition (SPAAC) method. The N$_3$-to-J591 and DFO-to-J591 ratios were roughly identical (2.8 chelators per antibody), showing that the click reaction was quantitative. This study was the first one combining click chemistry and site-specific approaches for the design of DFO immunoconjugates. The $^{89}$Zr−DFO−DIBO−GalNAz−J591 conjugate was shown to be as stable as the conventionally prepared $^{89}$Zr−DFO−NCS−J591 (>96% after 7 days incubation in serum); however, in vitro and in vivo studies demonstrated that both radioimmunoconjugates behaved in a nearly identical way. The same research group moved a step forward and prepared a site-specifically dual-labeled (PET−optical imaging [OI]) huA33, a mAb-targeting colorectal cancer.[49] In this case, the click-chemistry reaction was conducted with a mixture of DFO−DIBO and Alexa Fluor 680-DIBO, providing the hybrid imaging agents with different chelator-to-dye-to-mAb ratios (from 1:1.3:1 to 2.9:0.5:1). They used the same approach to design a PET−OI bimodal immunoconjugate based on a pancreatic ductal adenocarcinoma (PDAC) targeting antibody 5B1.[50]

These different conjugation strategies may result in different synthesis and radiolabeling efficiencies, but the linker chemistry may also change the stability of the radiolabeled bioconjugate,

**Table 1. Comparison of the Different $^{89}$Zr Chelators and Their Bifunctional Versions**

| Entry | Chelator | Bifunctional version (BFC) | Studies | Pros (+) and cons (-) |
|---|---|---|---|---|
| 1[52-53] | DFO* | DFO*-pPhe-NCS | - Conjugation of DFO* to bombesin<br>- Stability of $^{89}$Zr-DFO*-BBS by DFO challenging experiments<br>- Conjugation of DFO*-pPhe-NCS to trastuzumab, rituximab and cetuximab (pH 8.9-9.1, 30 min at 37°C, 2% DMSO, 0.6-0.8 chelator/mAb), and comparison with DFO-pPhe-NCS analogs<br>- Stability of $^{89}$Zr-DFO*-pPhe-NCS conjugates in human serum<br>- Biodistribution in N87 tumor-bearing mice<br>- PET imaging | + Higher stability / DFO<br>+ Similar tumor uptake but lower bone uptake of $^{89}$Zr-DFO*-pPhe-NCS-trastuzumab vs $^{89}$Zr-DFO-pPhe-NCS-trastuzumab |
| 2[34] | DFO-Sq | DFO-Sq | - Comparison of the stability of $^{89}$Zr-DFO-Sq and $^{89}$Zr-DFO-pPhe-NCS by EDTA challenging experiments<br>- Conjugation of DFO-Sq to trastuzumab and rituximab (pH 9, rt, <1% DMSO, up to 4.5 chelators/mAb), and comparison with DFO-pPhe-NCS analog<br>- Biodistribution in SKOV3 and BT-474 tumor-bearing mice<br>- PET imaging | + Higher stability / DFO<br>+ Improved radiolabeling efficiency / DFO<br>+ No radiolytic cleavage of the linker<br>+ Reduced bone and liver uptake of $^{89}$Zr-DFO-Sq-trastuzumab vs $^{89}$Zr-DFO-pPhe-NCS-trastuzumab<br>+ High quality PET images |
| 3[54] | C5-C7 | No | - Stability of $^{89}$Zr-C5-C7 in human serum<br>- Comparison of the stability of $^{89}$Zr-C5-C7 and $^{89}$Zr-DFO by EDTA challenging experiments | + Higher stability of C7 / DFO<br>− Lower radiolabeling efficiency / DFO<br>− No bifunctional version reported so far |

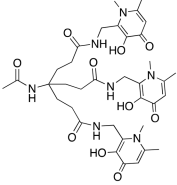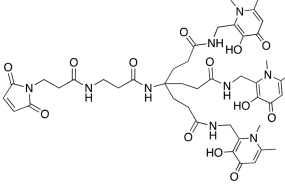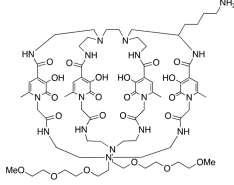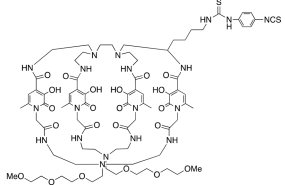| Entry | Chelator | Bifunctional version (BFC) | Studies | Pros and cons |
|---|---|---|---|---|
| 4[55] | R = H: FSC<br>R = COCH$_3$: TAFC | Accessible from the three primary amino groups of FSC | - Comparison of the stability of $^{89}$Zr-TAFC and $^{89}$Zr-DFO by EDTA and DFO challenging experiments<br>- Conjugation of FSC to three RGD peptides (pH 8, 30 min at rt, 16% MeCN)<br>- Stability of $^{89}$Zr-FSC conjugate by EDTA challenging experiments<br>- Biodistribution in M21 tumor-bearing mice<br>- PET imaging | + Higher stability / DFO<br>− Need for Fe$^{3+}$ complexation prior to conjugation<br>− Only 6 donor atoms<br>− 3 conjugation sites not suitable for conjugation to an antibody |
| 5[56] | L1: n=1, R = CH$_2$CONOHCH$_3$<br>L2: n=2, R = H<br>L3: n=2, R = CH$_2$CONOHCH$_3$<br>L4 | L5 | - Comparison of the stability of $^{89}$Zr-L1-L4 and $^{89}$Zr-DFO by EDTA challenging experiments<br>- Comparison of the biodistribution of $^{89}$Zr-L4 and $^{89}$Zr-DFO in Balb/C mice<br>- Conjugation of L5 to trastuzumab (pH 9.5, 2 h at rt, MeCN, 0.17 chelator/mAb) and comparison with DFO analog<br>- Biodistribution in BT-474 tumor-bearing mice<br>- PET imaging | − Lower conjugation efficiency / DFO<br>− Need for Fe$^{3+}$ complexation prior to conjugation<br>− Higher bone uptake of $^{89}$Zr-L4 and $^{89}$Zr-L5-trastuzumab vs $^{89}$Zr-DFO-trastuzumab |
| 6[57-58] | HOPO | HOPO-NCS | - Comparison of the stability of $^{89}$Zr-HOPO and $^{89}$Zr-DFO by EDTA challenging and metal competition experiments<br>- Conjugation of HOPO-NCS to trastuzumab (pH 8.5-9.0, 1.2% DMSO, 2.8 chelators/mAb) and comparison with DFO-pPhe-NCS analog<br>- Stability of $^{89}$Zr-HOPO and $^{89}$Zr-HOPO conjugate in human serum<br>- Biodistribution in BT-474 tumor-bearing mice<br>- PET imaging | + Higher stability / DFO<br>+ Much lower bone uptake of $^{89}$Zr-HOPO-NCS-trastuzumab vs $^{89}$Zr-DFO-pPhe-NCS-trastuzumab<br>− Lower tumor uptake of $^{89}$Zr-HOPO-NCS-trastuzumab vs $^{89}$Zr-DFO-pPhe-NCS-trastuzumab |

## Table 1. continued
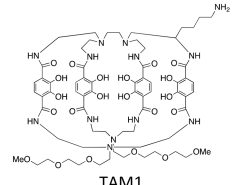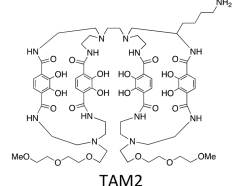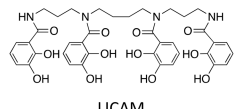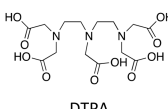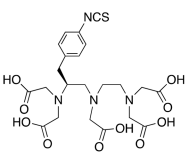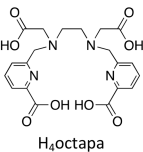
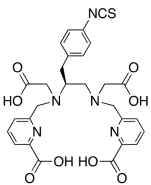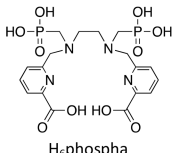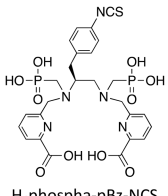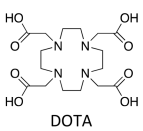| Entry | Chelator | Bifunctional version (BFC) | Studies | Pros and cons |
|---|---|---|---|---|
| 7[40] | <br>CP256 | <br>YM103 | - Transchelation experiments between $^{89}$Zr-CP256 and $^{89}$Zr-DFO<br>- Comparison of the stability of CP256 and DFO in the presence of Fe$^{3+}$<br>- Conjugation of YM103 to trastuzumab (30 min at 37°C, 2.3% DMSO, 4-8 chelators/mAb) and comparison with DFO-Mal analog<br>- Stability of $^{89}$Zr-YM103-trastuzumab and $^{89}$Zr-DFO-Mal-tratsuzumab conjugate in human serum<br>- Biodistribution in normal mice<br>- PET imaging | + Higher thermodynamic stability of $^{89}$Zr-CP256 vs $^{89}$Zr-DFO<br>− Lower conjugation efficiency / DFO-Mal<br>− Lower radiolabeling efficiency<br>− Lower stability of CP256 in the presence of Fe$^{3+}$<br>− Much higher bone uptake of $^{89}$Zr-YM103-trastuzumab vs $^{89}$Zr-DFO-Mal-trastuzumab: lower in vivo stability |
| 8[59] | <br>2,3-HOPO | <br>2,3-HOPO-pPhe-NCS | - Comparison of the stability of $^{89}$Zr-2,3-HOPO and $^{89}$Zr-DFO by DTPA challenging experiments<br>- Conjugation of 2,3-HOPO-pPhe-NCS to trastuzumab (pH 8.5, 90 min at 37°C, 10% DMF, 1.7 chelator/mAb) and an anti-gD mAb, and comparison with DFO-N-Suc-TFP analogs<br>- Stability of $^{89}$Zr-2,3-HOPO and $^{89}$Zr-2,3-HOPO-pPhe-NCS-trastuzumab in serum<br>- Biodistribution in SKOV3 tumor-bearing mice<br>- PET imaging | + Higher stability / DFO<br>− Lower stability in serum<br>− Slightly higher bone and liver uptake of $^{89}$Zr-2,3-HOPO-pPhe-NCS-mAb vs $^{89}$Zr-DFO-N-Suc-TFP-mAb |

| Entry | Chelator | Bifunctional version (BFC) | Studies | Pros and cons |
|---|---|---|---|---|
| 9[60] | <br>TAM1<br><br>TAM2 | Easily accessible from the primary amino group | - Comparison of the stability of $^{89}$Zr-TAM1-2 and $^{89}$Zr-DFO by DTPA challenging experiments<br>- Stability of $^{89}$Zr-TAM1-2 in human serum<br>- Biodistribution of $^{89}$Zr-TAM1 in normal mice | + Higher stability / DFO<br>− Higher liver and kidney uptake of $^{89}$Zr-TAM1 / $^{89}$Zr-DFO |
| 10[58] | <br>LICAM | No | - Radiolabeling experiments | − Low radiolabeling efficiency (< 30%) |
| 11[61] | <br>DTPA | <br>DTPA-pBz-NCS | - Conjugation of DTPA-pBz-NCS to Zevalin | − No radiolabeling (< 0.1%) |

**Table 1. continued**

| Entry | Chelator | Bifunctional version (BFC) | Studies | Pros and cons |
|---|---|---|---|---|
| 12[62] | H$_4$octapa | H$_4$octapa-pBz-NCS | - Radiolabeling experiments | − No radiolabeling |
| 13[63] | H$_6$phospha | H$_6$phospha-pBz-NCS | - Conjugation of H$_6$phospha-pBz-NCS to trastuzumab (pH 8.5-9.0, 1 h at 37°C, 2.4% DMSO, 3.3 chelators /mAb)<br>- Radiolabeling experiments | − Low radiolabeling efficiency (max 12%) |
| 14[64] | DOTA | Numerous DOTA-based BFC are available | - Radiolabeling experiments<br>- Comparison of the stability of $^{89}$Zr-DOTA and $^{89}$Zr-DFO by EDTA challenging experiments<br>- Comparison of the stability of $^{89}$Zr-DOTA and $^{89}$Zr-DFO in competition studies with various metals<br>- Stability of $^{89}$Zr-DOTA in human serum<br>- Biodistribution of $^{89}$Zr-DOTA in normal mice | + Outstanding stability (DOTA outperforms all other chelators)<br><br>− High temperature needed for radiolabeling<br><br>− No in vivo studies with DOTA-BFC-conjugates |

its immunoreactivity, and biodistribution and, therefore, can impact the quality of the PET images. From the studies conducted so far with different DFO bifunctional chelating agents, it is not obvious to define the better methodology for the design of a DFO-based immunoconjugate, partly because it is also "antibody-dependent". Although it is the most commonly used nowadays, especially due to the fact that the bifunctional chelating agent is commercially available, the DFO−pPhe−NCS-based strategy is far from perfect. DFO−pPhe−NCS, as is most of the hydroxamate-based chelators, is poorly soluble in water, thus requiring careful handling during the conjugation step. Also, the formed thiourea bond is susceptible to radiation-induced cleavage, although this limitation may be overcome by avoiding the presence of chloride anions. There is also no clear evidence of the added value of site-specific conjugation in comparison to random labeling. In most of the studies comparing both approaches, the site-specifically modified antibody did not outperform the conjugates prepared by conventional routes. However, as stated by Zeglis, one can believe that with some antibodies, it will be highly preferable to use well-defined, chemically controlled constructs. The development of new site-specific bioconjugation methods, together with the increasing number of click-chemistry tools available, should lead to the construction of finely designed immunoconjugates exhibiting higher selectivity and efficiency. Such approaches will also facilitate the design of more-sophisticated conjugates in the future, e.g., PET−OI bimodal imaging agents or imageable ADC.

Despite its extensive use, which makes it the gold standard for $^{89}$Zr-immunoPET, DFO and its bifunctional versions suffer from some drawbacks. Beside the issues discussed above regarding the way the DFO is attached to the antibody, the chelating agent by itself is probably not the best ligand for $^{89}$Zr complexation, thus being responsible of metal release in vivo.

These issues prompted several groups to seek for improved $^{89}$Zr chelators in the last 3 years.

**Alternatives to DFO.** Although no crystal structure of the $^{89}$Zr−DFO complex has been reported so far, density functional theory (DFT) calculations predicted that the radiometal is complexed by the three hydroxamate groups of the linear hexadentate ligand and that the coordination sphere of the metal ion was saturated by two water molecules.[21] Thus, the highly oxophilic hard cation Zr$^{4+}$ is stabilized by the octacoordination of eight oxygen atoms. However, it has been hypothesized that DFO is not an ideal chelator for $^{89}$Zr because of the presence of only three hydroxamate groups and the need of additional water molecules to allow the saturation of the coordination sphere of Zr$^{4+}$. The search for more-efficient chelators has been logically oriented toward molecular constructs containing intrinsically eight oxygen donor atoms.

*Hydroxamate-Based Chelators (DFO Analogs).* Brechbiel and co-workers investigated the coordination chemistry of Zr$^{4+}$ with four bidentate hydroxamates ligands and reported the single crystal X-ray structure of the octa-coordinated complex.[51] Following this pioneering work, Patra et al. designed an extended DFO, so-called DFO*, by appending an extra hydroxamate group to commercial DFO (Table 1, entry 1).[52] DFO* can thus wrap around the metal to give an octadentate complex as predicted by DFT calculations. Vugts et al. prepared a bifunctional version of DFO* (DFO*−pPhe−NCS), which was conjugated to trastuzumab, and the resulting conjugate was compared to the DFO analog.[53] DFO* conjugate showed superior characteristics, both in vitro and in vivo. The biodistribution of the two $^{89}$Zr-radiolabeled mAbs into N87 tumor-bearing nude mice showed similar blood kinetics and tumor uptake at 24, 72, and 144 h post injection (p.i.). Most importantly, DFO* showed significantly lower uptake in bone and also in liver and spleen tissue at 144 h p.i. Moreover, the

ratio of $^{89}$Zr—DFO—trastuzumab over $^{89}$Zr—DFO*—trastuzumab in femur was 1.5 at 24 h p.i. and increased to 5 at 144 h p.i.

Similar to the DFO* approach, Donnelly and co-workers proposed to use a squaramide ester derivative of DFO (DFO—Sq, Figure 2) for conjugation to trastuzumab (Table 1, entry 2).[34] The presence of two oxygen atoms in the squaramide group is supposed to complete the coordination of the $Zr^{4+}$ ion. In vivo comparison of $^{89}$Zr—DFO—trastuzumab and $^{89}$Zr—DFOSq—trastuzumab also turned to the advantage of the new conjugate, which, after injection in SK-OV-3 xenograft-bearing mice, improved PET imaging and resulted in higher tumor-to-bone ratio. Although there is no evidence of octacoordination of the metal and the difference of the tumor-to-bone ratio is not as pronounced as it is in the case of DFO*, especially 96 h p.i., this new bifunctional version of DFO shows advantages compared to DFO—pPhe—NCS in terms of radiolabeling efficiency. The authors also claimed that the squarate bond is more stable than the thiourea bond. Further comparative studies will be necessary to prove the superiority of this promising DFO analog.

It is well-established that metal complexes with macrocyclic compounds show higher kinetic inertness in comparison to their linear analogs. Brechbiel and co-workers decided to combine this favorable feature of the macrocyclic structure with the presence of eight coordinating oxygen atoms and synthesized a series of macrocyclic chelators of various sizes containing four hydroxamate units through ring closure metathesis of the corresponding linear compounds (Table 1, entry 3).[54] The macrocycle with the larger cavity size (C7) gave a much-more-stable Zr complex than DFO. However, no bioconjugatable version of this promising chelator has been prepared yet. Decristoforo et al. also chose to take advantage of the expected higher stability of macrocyclic derivatives and investigated the properties of fusarinine C (FSC), a cyclic natural siderophore containing three hydroxamate groups and its triacetylated derivative (TAFC) (Table 1, entry 4).[55] Despite the presence of only six coordinating oxygen atoms, $^{89}$Zr—TAFC showed much-higher stability in comparison to $^{89}$Zr—DFO, evidenced by challenge experiments with a large excess of EDTA, thus demonstrating the added value of the cyclic structure versus the linear one. The three secondary amines on FSC allowed the conjugation of the chelator to three cyclic RGD peptides. However, a limitation of the use of this candidate for $^{89}$Zr-immunoPET is the presence of the three identical secondary amine functions, which make it difficult to conjugate it to only one antibody.

Boros and co-workers have chosen to use macrocyclic tetraamines, i.e. cyclen or cyclam, as a scaffold to bring hydroxamate arms in favorable conformation for optimal $^{89}$Zr coordination (Table 1, entry 5).[56] A series of cyclen and cyclam derivatives bearing three or four hydroxamate groups of various lengths, including a bifunctional version, have been prepared. Unfortunately, none of them showed significantly improved properties in comparison to DFO.

*Hydroxypyridinone-, Terephthalamide-, and Catecholate-Based Chelators.* An alternative to hydroxamate groups as bidentate oxygenated ligands are catecholate or hydroxypyridinone groups. In particular, 1-hydroxypyridin-2-one groups exhibit lower $pK_a$ values than catechol or hydroxamic acid and are deprotonated at physiological pH, thus offering hard oxygen atoms suitable for Zr coordination. In 2014, Lewis and co-workers, inspired by the work of Raymond in the field of actinide separation,[65] proposed a new $^{89}$Zr chelator based on

four 1-hydroxypyridin-2-one groups appended to a linear tetraamine, i.e. 3,4,3-(LI-1,2-HOPO), also called HOPO (Table 1, entry 6).[57] DFT calculations showed that the $Zr^{4+}$ is octacoordinated by HOPO. This coordination scheme has been confirmed by a crystal structure.[58] In their first paper, a comprehensive stability study has demonstrated that $^{89}$Zr—HOPO complex exhibited much higher stability than $^{89}$Zr—DFO. Indeed, ligand challenge experiments with 100-fold excess EDTA within a 5—8 pH range left the $^{89}$Zr—HOPO as >99% intact even after 7 days at 37 °C, while the significant release of $^{89}$Zr from DFO was observed. $^{89}$Zr—HOPO also showed a good stability upon transmetalation with a large range of metal cations (10-fold excess), although 17% of $^{89}$Zr was replaced by $Fe^{3+}$ after 7 days. However, only 39% of the $^{89}$Zr—DFO complex remained intact under the same conditions. This promising behavior prompted the authors to prepare a bifunctional version of HOPO bearing a benzyl NCS group, which enabled its bioconjugation to trastuzumab.[58] Surprisingly, $^{89}$Zr—HOPO—trastuzumab appeared to be slightly less stable than $^{89}$Zr—DFO—trastuzumab in serum, but in vivo studies in BT474 xenograft-bearing mice confirmed the superiority of the new conjugate, especially regarding bone uptake. Indeed, after 336 h p.i., the tumor-to-bone ratio was more than 3-fold higher in the case of $^{89}$Zr—HOPO—trastuzumab.

Ma et al. used a tripodal ligand incorporating three 1,6-dimethyl-3-hydroxypyridin-4-one as $^{89}$Zr chelator (Table 1, entry 7).[40] This chelator, designated as CP256 or THP, has proven to be very effective for $^{68}$Ga labeling. A bifunctional derivative of CP256 containing a maleimide group (YM103) has been conjugated to trastuzumab after reducing mAb disulfide bonds and compared to a DFO analog. Both competition studies between DFO and CP256 and in vivo experiments in healthy mice (29% ID/g in bones after 3 days) led to the conclusion that this tripodal hexadentate chelator forms less stable complexes with $^{89}$Zr than DFO.

Another hydroxypyridinone isomer, i.e. 3-hydroxypyridin-2-one, has been investigated by Tinianow et al. (Table 1, entry 8).[59] A sophisticated macrobicyclic octadentate compound incorporating four 3-hydroxypyridin-2-one groups and a pPhe—NCS function was conjugated to trastuzumab and compared to the DFO analog in vivo in SK-OV-3 tumor bearing mice. The new bioconjugate showed slightly higher uptake in bone and liver compared to the DFO analog. The authors expect that changing the topology of the chelator and, thus, the positioning of the 3-hydroxypyridin-2-one groups could lead to more stable complexes. The same research group has also prepared a pair of structural analogs incorporating four terephthalamide groups instead of hydroxypyridinones TAM1 and TAM2 (Table 1, entry 9).[60] The corresponding $^{89}$Zr complexes exhibited higher stability in vitro than DFO as evidenced by challenge experiments with excess DTPA and comparable bone uptake after injection in normal mice. However, the liver and kidney uptake of the new complexes were higher than those of $^{89}$Zr—DFO. These chelators have not been conjugated to a biomolecule.

A catechol containing analog of HOPO (LICAM) has been investigated by Lewis and co-workers (Table 1, entry 10) but was found to be inefficient for $^{89}$Zr complexation (maximum radiochemical yield of <30%), probably due to the too-high $pK_a$ value of the catechol group.[58]

*Carboxylate- and Phosphonate-Based Chelators.* Diethylenetriaminepentaacetic acid (DTPA) was proven to be a poor

candidate for $^{89}$Zr labeling after bioconjugation of a bifunctional derivative, DTPA−pBz−NCS, to Zevalin (anti-CD20), with a labeling yield of <0.1% (Table 1, entry 11).[61] Orvig and co-workers investigated another acyclic chelator containing carboxylate functions designed for $^{111}$In labeling, H$_4$octapa (Table 1, entry 12), but their attempts to radiolabel H$_4$octapa−-trastuzumab conjugate with $^{89}$Zr failed.[62] With the aim of improving radiolabeling kinetics, they chose to replace two carboxylate arms with two phosphonate groups. A bifunctional version of this chelator, H$_6$phospha−pBz−NCS (Table 1, entry 13), was conjugated to trastuzumab (3.3 chelators per antibody) and $^{89}$Zr radiolabeling experiments of the conjugate have confirmed their hypothesis. However, the maximum labeling yield (12%) compared poorly to the standard DFO.[63]

Finally, a very recent study from the Wadas research group could revolutionize the field (Table 1, entry 14−16).[64] Contrary to what was stated by many authors, it appeared that 1,4,7,10-tetraazacyclododecane-1,4,7,10-tetraacetic acid (DOTA) could be a powerful alternative to DFO for complexing $^{89}$Zr. DOTA is a workhorse chelator that shows extraordinary coordination properties for a wide range of metals including lanthanides (Gd-based contrast agents for MRI) and a large number of radioisotopes used for SPECT ($^{111}$In), PET ($^{64}$Cu, and $^{68}$Ga), or RIT ($^{177}$Lu, $^{90}$Y, and $^{225}$Ac). A tremendous number of studies has been devoted to tetraazacycloalkanes chemistry to finely tune the coordination properties toward a given metal, and different approaches have been devised to provide bifunctional versions of such derivatives for bio-conjugation to various biovectors.[66−69] Surprisingly, this highly versatile family of chelators remained largely unexplored for Zr complexation, based on the well-reasoned idea that their structure is not well-adapted to the highly oxophilic Zr$^{4+}$ hard cation. Indeed, the presence of only four hard donor oxygen atoms and four nitrogen atoms in DOTA was believed to give less-stable Zr complexes than the ones in which the metal is surrounded by eight oxygen atoms. In their paper, Wadas and co-workers reported for the first time the single crystal structure of Zr−DOTA, which is typical of a DOTA metal complex, i.e. the metal cation is entrapped in the cage and octacoordinated by the four nitrogen atoms of the cyclic scaffold and the four oxygen atoms of the acetate pendant arms. A comprehensive stability study of $^{89}$Zr−DOTA has been performed, demon-strating an excellent stability of the complex. DOTA clearly outperformed all its competitors, including DFO. It also showed exceptional in vivo behavior, with much less liver, kidney, and bone uptake than $^{89}$Zr−DFO. Will DOTA replace DFO and end the quest for improved Zr chelators? Probably not, because DOTA suffers from one major drawback. As a counterpart of its exceptional and unexpected kinetic inertness, the formation of the $^{89}$Zr−DOTA complex requires conditions, which are not compatible with biovectors such as antibodies. Indeed, 100% incorporation of the radiometal could be reached only after heating at 95 °C during 1 h with $^{89}$ZrCl$_4$. $^{89}$ZrCl$_4$ was preferred to $^{89}$Zr(ox)$_2$, which gave only 65% radiochemical yield after 2h at 99 °C, while the radiometalation of DFO was quantitative at room temperature within 15 min. This is also an issue because $^{89}$ZrCl$_4$ has to be prepared starting from commercially available $^{89}$Zr(ox)$_2$ prior to radiometalation; however, it is known that $^{89}$ZrCl$_4$ is preferred to $^{89}$Zr(ox)$_2$ for toxicity reasons. If the conditions needed for the incorporation of $^{89}$Zr into DOTA obviously prohibit the use of this chelator for $^{89}$Zr-immunoPET in a conventional way, i.e.,

the first bioconjugation and then radiometalation in the last step, this work opens the door to a hot-conjugation approach, preparing the $^{89}$Zr complex of a bifunctional DOTA prior to the bioconjugation step. Although not optimal, this approach may be facilitated by the easy access to a wide range of bifunctional DOTA derivatives and the development of numerous efficient click-chemistry methods for bioconjugation. No doubt that such approach will be investigated in the future and if the gain in stability is demonstrated by in vivo studies and overcomes the less-straightforward labeling procedures, then DOTA could become a serious candidate for $^{89}$Zr-immunoPET. It is also a valuable alternative for biomolecules that can resist the high temperatures required for the incorporation of $^{89}$Zr into the DOTA macrocycle.

## ■ CONCLUSIONS AND FUTURE DEVELOPMENTS

From the studies reported so far, it is evident that numerous parameters may affect the labeling efficiency, stability, and biodistribution of $^{89}$Zr-labeled immunoconjugates: the coordi-nation properties of the chelator, the nature of the linker, the way the probe is conjugated to the antibody. It is not obvious to claim which combination of these different factors will be the best, particularly because it may also depend on the nature of the antibody. However, some trends can be drawn from the work done so far.

Regarding the bioconjugation method, routinely used approaches, e.g., involving isothiocyanate or maleimide functions to conjugate, respectively, to lysines or cysteines residues, may not be ideal. Indeed, the resulting bonds linking the $^{89}$Zr complex to the biomolecule may be partially cleaved in some cases. Some recent alternatives are appealing. For instance, among the bifunctional DFO derivatives, DFO−Sq showed interesting behavior; however, the promising properties of this BFC need to be validated in subsequent studies. More importantly, one may predict that further improvements will arise from rapid advances in the field of site-specific bioconjugation and click-chemistry. The right combination of a site-specific bioconjugation method and a bioorthogonal reaction should lead to better-defined and stable constructs with higher immunoreactivity. Moreover, these powerful tools, allowing the fine chemical control of the biomolecule modification, will facilitate the design of bimodal imaging (PET−OI) and theranostic agents (imageable ADC), which undoubtedly represent the next generation of immunoconju-gates.

It is now generally accepted that DFO is not the best chelator for $^{89}$Zr, although (to different levels) bone uptake was observed in all in vivo experiments whatever the DFO-based BFC used. This concern prompted many groups to develop new chelators with improved $^{89}$Zr coordination properties. Some of them failed because they were proven to be less efficient than DFO; none of them are perfect, but all of this recent work (in the last three years) has helped to better understand the important features that a good candidate must meet. First, it is clear that eight donor atoms, preferentially oxygen atoms, are necessary to complete the coordination sphere around the Zr$^{4+}$ metal ion. Thus, extended DFO, such as DFO* or DFO−Sq, proved to be superior to DFO in many aspects, although they still suffer from some drawbacks such as poor water solubility or lower radiolabeling efficiency. Among the alternatives to hydroxamate group that have been evaluated, hydroxypyridinone is probably the most promising one, with HOPO and, to a lesser extent, 2,3-HOPO showing higher in

vitro and in vivo properties in comparison to DFO. The well-known macrocyclic effect could also play an important role in improving the [89]Zr complex stability, but the synthesis of chelators incorporating in the macrocyclic ring four hydroxamate or hydroxypyridinone moieties is not straightforward, and the preparation of their bifunctional versions is even more difficult. Finally, DOTA is definitely an option that need to be investigated further despite the high temperature required for complexation. The long half-life of [89]Zr allows the metalation to be carried out prior to the bioconjugation step, providing that a good kit that is easy to conjugate is developed.

It appears from the recent advances in the field that there is still room for improved chelators and novel bioconjugation approaches to facilitate the development of ever-more-efficient [89]Zr immunoconjugates. However, these radioimmunoconjugates will have to demonstrate clear superiority in subsequent preclinical and clinical studies in comparison to the first generation of [89]Zr immunoconjugates that are now widely used for many clinical applications. The cost of development of these new [89]Zr immunoconjugates will have to be taken into account. The use of new bifunctional chelating agents, if proven to be significantly better than commercially available DFO derivatives, should not impair too much the global cost of the radioimmunoconjugate. The strategies involving engineering of mAb prior to the bioconjugation step could have a stronger financial impact, and the added value of such immunoconjugates compared to the ones prepared by conventional routes will have to be high, which was not clearly demonstrated so far. However, the recent development for clinical applications of site-specifically constructed ADC indicates that this approach is worth being further investigated.

## ■ AUTHOR INFORMATION

**Corresponding Author**
*E-mail: franck.denat@u-bourgogne.fr.

**ORCID** ⓘ
Sandra Heskamp: 0000-0001-7250-0846

**Notes**
The authors declare the following competing financial interest(s): Franck Denat is a scientific advisor in Chematech.

## ■ ABBREVIATIONS

ADC, antibody-drug conjugate; BFC, bifunctional chelator; BODIPY, boron—dipyrromethene; BTG, bacterial transglutaminase; CT, computed tomography; DFO, desferrioxamine; DFT, density functional theory; DIBO, dibenzocyclooctyne; DOTA, 1,4,7,10-tetraazacyclododecane-1,4,7,10-tetraacetic acid; DTPA, diethylenetriaminepentaacetic acid; EDTA, ethylenediaminetetraacetic acid; EGFR, epidermal growth factor receptor; EpCam, epithelial cell adhesion molecule; FDG, fluorodeoxyglucose; GalNaz, N-azidoacetylgalactosamine; HNSCC, head and neck squamous cell carcinoma; HSP, heat-shock protein; ID, injected dose; IEDDA, inverse electron

demand Diels—Alder reaction; mAb, monoclonal antibody; MRI, magnetic resonance imaging; NHS, N-hydroxysuccinimide; OI, optical imaging; PBS, phosphate-buffered saline; PDAC, pancreatic ductal adenocarcinoma; PET, positron emission tomography; PSMA, prostate-specific membrane antigen; SATA, N-succinimidyl—S-acetylthioacetate; SMCC, succinimidyl 4-(N-maleimidomethyl)cyclohexane-1-carboxylate; SPAAC, strain-promoted alkyne—azide cycloaddition; SPECT, single photon emission computed tomography; TCEP, Tris(2-carboxyethyl)phosphine; TCO, transcyclooctene; TFP, tetrafluorophenol; VEGF, vascular endothelial growth factor

## ■ REFERENCES

(1) Borjesson, P. K., Jauw, Y. W., Boellaard, R., de Bree, R., Comans, E. F., Roos, J. C., Castelijns, J. A., Vosjan, M. J., Kummer, J. A., Leemans, C. R., et al. (2006) Performance of immuno-positron emission tomography with zirconium-89-labeled chimeric monoclonal antibody U36 in the detection of lymph node metastases in head and neck cancer patients. *Clin. Cancer Res. 12*, 2133—2140.

(2) Dijkers, E. C., Oude Munnink, T. H., Kosterink, J. G., Brouwers, A. H., Jager, P. L., de Jong, J. R., van Dongen, G. A., Schroder, C. P., Lub-de Hooge, M. N., and de Vries, E. G. (2010) Biodistribution of 89Zr-trastuzumab and PET imaging of HER2-positive lesions in patients with metastatic breast cancer. *Clin. Pharmacol. Ther. 87*, 586—592.

(3) Pandit-Taskar, N., O'Donoghue, J. A., Durack, J. C., Lyashchenko, S. K., Cheal, S. M., Beylergil, V., Lefkowitz, R. A., Carrasquillo, J. A., Martinez, D. F., Fung, A. M., et al. (2015) A Phase I/II Study for Analytic Validation of 89Zr-J591 ImmunoPET as a Molecular Imaging Agent for Metastatic Prostate Cancer. *Clin. Cancer Res. 21*, 5277—5285.

(4) van Es, S. C., Brouwers, A. H., Mahesh, S. V. K., Leliveld-Kors, A. M., de Jong, I. J., Lub-de Hooge, M. N., de Vries, E. G. E., Gietema, J. A., and Oosting, S. F. (2017) 89Zr-Bevacizumab PET: Potential Early Indicator of Everolimus Efficacy in Patients with Metastatic Renal Cell Carcinoma. *J. Nucl. Med. 58*, 905—910.

(5) Gaykema, S. B., Brouwers, A. H., Hovenga, S., Lub-de Hooge, M. N., de Vries, E. G., and Schroder, C. P. (2012) Zirconium-89-trastuzumab positron emission tomography as a tool to solve a clinical dilemma in a patient with breast cancer. *J. Clin. Oncol. 30*, e74—75.

(6) Gebhart, G., Lamberts, L. E., Wimana, Z., Garcia, C., Emonts, P., Ameye, L., Stroobants, S., Huizing, M., Aftimos, P., Tol, J., et al. (2016) Molecular imaging as a tool to investigate heterogeneity of advanced HER2-positive breast cancer and to predict patient outcome under trastuzumab emtansine (T-DM1): the ZEPHIR trial. *Ann. Oncol. 27*, 619—624.

(7) Desar, I. M., Stillebroer, A. B., Oosterwijk, E., Leenders, W. P., van Herpen, C. M., van der Graaf, W. T., Boerman, O. C., Mulders, P. F., and Oyen, W. J. (2010) 111In-bevacizumab imaging of renal cell cancer and evaluation of neoadjuvant treatment with the vascular endothelial growth factor receptor inhibitor sorafenib. *J. Nucl. Med. 51*, 1707—1715.

(8) Heskamp, S., Boerman, O. C., Molkenboer-Kuenen, J. D., Oyen, W. J., van der Graaf, W. T., and van Laarhoven, H. W. (2013) Bevacizumab reduces tumor targeting of anti-epidermal growth factor and anti-insulin-like growth factor 1 receptor antibodies. *Int. J. Cancer 133*, 307.

(9) Pastuskovas, C. V., Mundo, E. E., Williams, S. P., Nayak, T. K., Ho, J., Ulufatu, S., Clark, S., Ross, S., Cheng, E., Parsons-Reponte, K., et al. (2012) Effects of anti-VEGF on pharmacokinetics, biodistribution and tumor penetration of trastuzumab in a preclinical breast cancer model. *Mol. Cancer Ther. 11*, 752.

(10) Perk, L. R., Visser, G. W., Vosjan, M. J., Stigter-van, W. M., Tijink, B. M., Leemans, C. R., and van Dongen, G. A. (2005) (89)Zr as a PET surrogate radioisotope for scouting biodistribution of the therapeutic radiometals (90)Y and (177)Lu in tumor-bearing nude

mice after coupling to the internalizing antibody cetuximab. *J. Nucl. Med. 46*, 1898−1906.

(11) Rizvi, S. N., Visser, O. J., Vosjan, M. J., van Lingen, A., Hoekstra, O. S., Zijlstra, J. M., Huijgens, P. C., van Dongen, G. A., and Lubberink, M. (2012) Biodistribution, radiation dosimetry and scouting of 90Y-ibritumomab tiuxetan therapy in patients with relapsed B-cell non-Hodgkin's lymphoma using 89Zr-ibritumomab tiuxetan and PET. *Eur. J. Nucl. Med. Mol. Imaging 39*, 512−520.

(12) Verel, I., Visser, G. W. M., Boerman, O. C., van Eerd, J. E. M., Finn, R., Boellaard, R., Vosjan, M. J. W. D., Stigter-van Walsum, M., Snow, G. B., and van Dongen, G. E. M. (2003) Long-Lived Positron Emitters Zirconium-89 and Iodine-124 for Scouting of Therapeutic Radioimmunoconjugates with PET. *Cancer Biother.Radiopharm. 18*, 655−661.

(13) Meijs, W. E., Haisma, H. J., Klok, R. P., van Gog, F. B., Kievit, E., Pinedo, H. M., and Herscheid, J. D. (1997) Zirconium-labeled monoclonal antibodies and their distribution in tumor-bearing nude mice. *J. Nucl. Med. 38*, 112−118.

(14) Jauw, Y. W., Menke-van der Houven van Oordt, C. W., Hoekstra, O. S., Hendrikse, N. H., Vugts, D. J., Zijlstra, J. M., Huisman, M. C., and van Dongen, G. A. (2016) Immuno-Positron Emission Tomography with Zirconium-89-Labeled Monoclonal Antibodies in Oncology: What Can We Learn from Initial Clinical Trials? *Front. Pharmacol. 7*, 131.

(15) Deri, M. A., Zeglis, B. M., Francesconi, L. C., and Lewis, J. S. (2013) PET imaging with 89Zr: From radiochemistry to the clinic. *Nucl. Med. Biol. 40*, 3−14.

(16) Gaykema, S. B., Schroder, C. P., Vitfell-Rasmussen, J., Chua, S., Oude Munnink, T. H., Brouwers, A. H., Bongaerts, A. H., Akimov, M., Fernandez-Ibarra, C., Lub-de Hooge, M. N., et al. (2014) 89Zr-trastuzumab and 89Zr-bevacizumab PET to evaluate the effect of the HSP90 inhibitor NVP-AUY922 in metastatic breast cancer patients. *Clin. Cancer Res. 20*, 3945−3954.

(17) van de Watering, F. C., Rijpkema, M., Perk, L., Brinkmann, U., Oyen, W. J., and Boerman, O. C. (2014) Zirconium-89 labeled antibodies: a new tool for molecular imaging in cancer patients. *BioMed Res. Int. 2014*, 203601.

(18) Lamberts, L. E., Williams, S. P., Terwisscha van Scheltinga, A. G., Lub-de Hooge, M. N., Schroder, C. P., Gietema, J. A., Brouwers, A. H., and de Vries, E. G. (2015) Antibody positron emission tomography imaging in anticancer drug development. *J. Clin. Oncol. 33*, 1491−1504.

(19) Dijkers, E. C., Kosterink, J. G., Rademaker, A. P., Perk, L. R., van Dongen, G. A., Bart, J., de Jong, J. R., de Vries, E. G., and Lub-de Hooge, M. N. (2009) Development and characterization of clinical-grade 89Zr-trastuzumab for HER2/neu immunoPET imaging. *J. Nucl. Med. 50*, 974−981.

(20) Heskamp, S., van Laarhoven, H. W., Molkenboer-Kuenen, J. D., Franssen, G. M., Versleijen-Jonkers, Y. M., Oyen, W. J., van der Graaf, W. T., and Boerman, O. C. (2010) ImmunoSPECT and immunoPET of IGF-1R expression with the radiolabeled antibody R1507 in a triple-negative breast cancer model. *J. Nucl. Med. 51*, 1565−1572.

(21) Holland, J. P., Divilov, V., Bander, N. H., Smith-Jones, P. M., Larson, S. M., and Lewis, J. S. (2010) 89Zr-DFO-J591 for immunoPET of prostate-specific membrane antigen expression in vivo. *J. Nucl. Med. 51*, 1293−1300.

(22) Laverman, P., van der Geest, T., Terry, S. Y., Gerrits, D., Walgreen, B., Helsen, M. M., Nayak, T. K., Freimoser-Grundschober, A., Waldhauer, I., Hosse, R. J., et al. (2015) Immuno-PET and Immuno-SPECT of Rheumatoid Arthritis with Radiolabeled Anti-Fibroblast Activation Protein Antibody Correlates with Severity of Arthritis. *J. Nucl. Med. 56*, 778−783.

(23) Price, T. W., Greenman, J., and Stasiuk, G. J. (2016) Current advances in ligand design for inorganic positron emission tomography tracers 68Ga, 64Cu, 89Zr and 44Sc. *Dalton Trans. 45*, 15702−15724.

(24) Brasse, D., and Nonat, A. (2015) Radiometals: towards a new success story in nuclear imaging? *Dalton Trans. 44*, 4845−4858.

(25) Zeglis, B. M., Houghton, J. L., Evans, M. J., Viola-Villegas, N., and Lewis, J. S. (2014) Underscoring the Influence of Inorganic Chemistry on Nuclear Imaging with Radiometals. *Inorg. Chem. 53*, 1880−1899.

(26) Price, E. W., and Orvig, C. (2014) Matching chelators to radiometals for radiopharmaceuticals. *Chem. Soc. Rev. 43*, 260−290.

(27) Adumeau, P., Sharma, S. K., Brent, C., and Zeglis, B. M. (2016) Site-Specifically Labeled Immunoconjugates for Molecular Imaging–Part 2: Peptide Tags and Unnatural Amino Acids. *Mol. Imaging Biol. 18*, 153−165.

(28) Adumeau, P., Sharma, S. K., Brent, C., and Zeglis, B. M. (2016) Site-Specifically Labeled Immunoconjugates for Molecular Imaging–Part 1: Cysteine Residues and Glycans. *Mol. Imaging Biol. 18*, 1−17.

(29) Vugts, D. J., Visser, G. W. M., and van Dongen, G. A. M. S. (2013) 89Zr-PET Radiochemistry in the Development and Application of Therapeutic Monoclonal Antibodies and Other Biologicals. *Curr. Top. Med. Chem. 13*, 446−457.

(30) Fischer, G., Seibold, U., Schirrmacher, R., Wängler, B., and Wängler, C. (2013) 89Zr, a Radiometal Nuclide with High Potential for Molecular Imaging with PET: Chemistry, Applications and Remaining Challenges. *Molecules 18*, 6469−6490.

(31) Meijs, W. E., Herscheid, J. D. M., Haisma, H. J., and Pinedo, H. M. (1992) Evaluation of desferal as a bifunctional chelating agent for labeling antibodies with Zr-89. *Int. J. Rad Appl. Instrum A 43*, 1443−1447.

(32) Verel, I., Visser, G. W., Boellaard, R., Stigter-van, W. M., Snow, G. B., and van Dongen, G. A. (2003) 89Zr immuno-PET: comprehensive procedures for the production of 89Zr-labeled monoclonal antibodies. *J. Nucl. Med. 44*, 1271−1281.

(33) Perk, L. R., Vosjan, M. J. W. D., Visser, G. W. M., Budde, M., Jurek, P., Kiefer, G. E., and van Dongen, G. A. M. S. (2010) p-Isothiocyanatobenzyl-desferrioxamine: a new bifunctional chelate for facile radiolabeling of monoclonal antibodies with zirconium-89 for immuno-PET imaging. *Eur. J. Nucl. Med. Mol. Imaging 37*, 250−259.

(34) Rudd, S. E., Roselt, P., Cullinane, C., Hicks, R. J., and Donnelly, P. S. (2016) A desferrioxamine B squaramide ester for the incorporation of zirconium-89 into antibodies. *Chem. Commun. 52*, 11889−11892.

(35) Sijbrandi, N. J., Merkul, E., Muns, J. A., Waalboer, D. C. J., Adamzek, K., Bolijn, M., Montserrat, V., Somsen, G. W., Haselberg, R., Steverink, P. J. G. M., et al. (2017) A Novel Platinum(II)−Based Bifunctional ADC Linker Benchmarked Using 89Zr-Desferal and Auristatin F−Conjugated Trastuzumab. *Cancer Res. 77*, 257.

(36) Zeglis, B. M., Mohindra, P., Weissmann, G. I., Divilov, V., Hilderbrand, S. A., Weissleder, R., and Lewis, J. S. (2011) Modular Strategy for the Construction of Radiometalated Antibodies for Positron Emission Tomography Based on Inverse Electron Demand Diels−Alder Click Chemistry. *Bioconjugate Chem. 22*, 2048−2059.

(37) Zeglis, B. M., Emmetiere, F., Pillarsetty, N., Weissleder, R., Lewis, J. S., and Reiner, T. (2014) Building Blocks for the Construction of Bioorthogonally Reactive Peptides via Solid-Phase Peptide Synthesis. *ChemistryOpen 3*, 48−53.

(38) Vugts, D. J., Vervoort, A., Stigter-van Walsum, M., Visser, G. W., Robillard, M. S., Versteegen, R. M., Vulders, R. C., Herscheid, J. K., and van Dongen, G. A. (2011) Synthesis of phosphine and antibody-azide probes for in vivo Staudinger ligation in a pretargeted imaging and therapy approach. *Bioconjugate Chem. 22*, 2072−2081.

(39) Tinianow, J. N., Gill, H. S., Ogasawara, A., Flores, J. E., Vanderbilt, A. N., Luis, E., Vandlen, R., Darwish, M., Junutula, J. R., Williams, S.-P., et al. (2010) Site-specifically 89Zr-labeled monoclonal antibodies for ImmunoPET. *Nucl. Med. Biol. 37*, 289−297.

(40) Ma, M. T., Meszaros, L. K., Paterson, B. M., Berry, D. J., Cooper, M. S., Ma, Y., Hider, R. C., and Blower, P. J. (2015) Tripodal tris(hydroxypyridinone) ligands for immunoconjugate PET imaging with 89Zr4+: comparison with desferrioxamine-B. *Dalton Trans. 44*, 4884−4900.

(41) Zeglis, B. M., Davis, C. B., Aggeler, R., Kang, H. C., Chen, A., Agnew, B. J., and Lewis, J. S. (2013) Enzyme-Mediated Methodology for the Site-Specific Radiolabeling of Antibodies Based on Catalyst-Free Click Chemistry. *Bioconjugate Chem. 24*, 1057−1067.

(42) Vosjan, M. J. W. D., Perk, L. R., Visser, G. W. M., Budde, M., Jurek, P., Kiefer, G. E., and van Dongen, G. A. M. S. (2010) Conjugation and radiolabeling of monoclonal antibodies with zirconium-89 for PET imaging using the bifunctional chelate p-isothiocyanatobenzyl-desferrioxamine. *Nat. Protoc. 5*, 739−743.

(43) Meyer, J.-P., Adumeau, P., Lewis, J. S., and Zeglis, B. M. (2016) Click Chemistry and Radiochemistry: The First 10 Years. *Bioconjugate Chem. 27*, 2791−2807.

(44) Meimetis, L. G., Boros, E., Carlson, J. C., Ran, C., Caravan, P., and Weissleder, R. (2016) Bioorthogonal Fluorophore Linked DFO—Technology Enabling Facile Chelator Quantification and Multimodal Imaging of Antibodies. *Bioconjugate Chem. 27*, 257−263.

(45) Agarwal, P., and Bertozzi, C. R. (2015) Site-Specific Antibody−Drug Conjugates: The Nexus of Bioorthogonal Chemistry, Protein Engineering, and Drug Development. *Bioconjugate Chem. 26*, 176−192.

(46) Merten, H., Brandl, F., Plückthun, A., and Zangemeister-Wittke, U. (2015) Antibody−Drug Conjugates for Tumor Targeting—Novel Conjugation Chemistries and the Promise of non-IgG Binding Proteins. *Bioconjugate Chem. 26*, 2176−2185.

(47) Jeger, S., Zimmermann, K., Blanc, A., Grünberg, J., Honer, M., Hunziker, P., Struthers, H., and Schibli, R. (2010) Site-Specific and Stoichiometric Modification of Antibodies by Bacterial Transglutaminase. *Angew. Chem., Int. Ed. 49*, 9995−9997.

(48) van Geel, R., Wijdeven, M. A., Heesbeen, R., Verkade, J. M. M., Wasiel, A. A., van Berkel, S. S., and van Delft, F. L. (2015) Chemoenzymatic Conjugation of Toxic Payloads to the Globally Conserved N-Glycan of Native mAbs Provides Homogeneous and Highly Efficacious Antibody−Drug Conjugates. *Bioconjugate Chem. 26*, 2233−2242.

(49) Zeglis, B. M., Davis, C. B., Abdel-Atti, D., Carlin, S. D., Chen, A., Aggeler, R., Agnew, B. J., and Lewis, J. S. (2014) Chemoenzymatic Strategy for the Synthesis of Site-Specifically Labeled Immunoconjugates for Multimodal PET and Optical Imaging. *Bioconjugate Chem. 25*, 2123−2128.

(50) Houghton, J. L., Zeglis, B. M., Abdel-Atti, D., Aggeler, R., Sawada, R., Agnew, B. J., Scholz, W. W., and Lewis, J. S. (2015) Site-specifically labeled CA19.9-targeted immunoconjugates for the PET, NIRF, and multimodal PET/NIRF imaging of pancreatic cancer. *Proc. Natl. Acad. Sci. U. S. A. 112*, 15850−15855.

(51) Guerard, F., Lee, Y.-S., Tripier, R., Szajek, L. P., Deschamps, J. R., and Brechbiel, M. W. (2013) Investigation of Zr(iv) and 89Zr(iv) complexation with hydroxamates: progress towards designing a better chelator than desferrioxamine B for immuno-PET imaging. *Chem. Commun. 49*, 1002−1004.

(52) Patra, M., Bauman, A., Mari, C., Fischer, C. A., Blacque, O., Haussinger, D., Gasser, G., and Mindt, T. L. (2014) An octadentate bifunctional chelating agent for the development of stable zirconium-89 based molecular imaging probes. *Chem. Commun. 50*, 11523−11525.

(53) Vugts, D. J., Klaver, C., Sewing, C., Poot, A. J., Adamzek, K., Huegli, S., Mari, C., Visser, G. W., Valverde, I. E., Gasser, G., et al. (2017) Comparison of the octadentate bifunctional chelator DFO*-pPhe-NCS and the clinically used hexadentate bifunctional chelator DFO-pPhe-NCS for 89Zr-immuno-PET. *Eur. J. Nucl. Med. Mol. Imaging 44*, 286−295.

(54) Guérard, F., Lee, Y.-S., and Brechbiel, M. W. (2014) Rational Design, Synthesis, and Evaluation of Tetrahydroxamic Acid Chelators for Stable Complexation of Zirconium(IV). *Chem. - Eur. J. 20*, 5584−5591.

(55) Zhai, C., Summer, D., Rangger, C., Franssen, G. M., Laverman, P., Haas, H., Petrik, M., Haubner, R., and Decristoforo, C. (2015) Novel Bifunctional Cyclic Chelator for 89Zr Labeling−Radiolabeling and Targeting Properties of RGD Conjugates. *Mol. Pharmaceutics 12*, 2142−2150.

(56) Boros, E., Holland, J. P., Kenton, N., Rotile, N., and Caravan, P. (2016) Macrocycle-Based Hydroxamate Ligands for Complexation and Immunoconjugation of 89Zirconium for Positron Emission Tomography (PET) Imaging. *ChemPlusChem 81*, 274−281.

(57) Deri, M. A., Ponnala, S., Zeglis, B. M., Pohl, G., Dannenberg, J. J., Lewis, J. S., and Francesconi, L. C. (2014) Alternative Chelator for 89Zr Radiopharmaceuticals: Radiolabeling and Evaluation of 3,4,3-(LI-1,2-HOPO). *J. Med. Chem. 57*, 4849−4860.

(58) Deri, M. A., Ponnala, S., Kozlowski, P., Burton-Pye, B. P., Cicek, H. T., Hu, C., Lewis, J. S., and Francesconi, L. C. (2015) p-SCN-Bn-HOPO: A Superior Bifunctional Chelator for 89Zr ImmunoPET. *Bioconjugate Chem. 26*, 2579−2591.

(59) Tinianow, J. N., Pandya, D. N., Pailloux, S. L., Ogasawara, A., Vanderbilt, A. N., Gill, H. S., Williams, S. P., Wadas, T. J., Magda, D., and Marik, J. (2016) Evaluation of a 3-hydroxypyridin-2-one (2,3-HOPO) Based Macrocyclic Chelator for 89Zr4+ and Its Use for ImmunoPET Imaging of HER2 Positive Model of Ovarian Carcinoma in Mice. *Theranostics 6*, 511−521.

(60) Pandya, D. N., Pailloux, S., Tatum, D., Magda, D., and Wadas, T. J. (2015) Di-macrocyclic terephthalamide ligands as chelators for the PET radionuclide zirconium-89. *Chem. Commun. 51*, 2301−2303.

(61) Perk, L. R., Visser, O. J., Stigter-van Walsum, M., Vosjan, M. J. W. D., Visser, G. W. M., Zijlstra, J. M., Huijgens, P. C., and van Dongen, G. A. M. S. (2006) Preparation and evaluation of 89Zr-Zevalin for monitoring of 90Y-Zevalin biodistribution with positron emission tomography. *Eur. J. Nucl. Med. Mol. Imaging 33*, 1337−1345.

(62) Price, E. W., Cawthray, J. F., Bailey, G. A., Ferreira, C. L., Boros, E., Adam, M. J., and Orvig, C. (2012) H4octapa: An Acyclic Chelator for 111In Radiopharmaceuticals. *J. Am. Chem. Soc. 134*, 8670−8683.

(63) Price, E. W., Zeglis, B. M., Lewis, J. S., Adam, M. J., and Orvig, C. (2014) H6phospa-trastuzumab: bifunctional methylenephosphonate-based chelator with 89Zr, 111In and 177Lu. *Dalton Trans. 43*, 119−131.

(64) Pandya, D. N., Bhatt, N., Yuan, H., Day, C. S., Ehrmann, B. M., Wright, M., Bierbach, U., and Wadas, T. J. (2017) Zirconium tetraazamacrocycle complexes display extraordinary stability and provide a new strategy for zirconium-89-based radiopharmaceutical development. *Chem. Sci. 8*, 2309−2314.

(65) Gorden, A. E. V., Xu, J., Raymond, K. N., and Durbin, P. (2003) Rational Design of Sequestering Agents for Plutonium and Other Actinides. *Chem. Rev. 103*, 4207−4282.

(66) Wängler, C., Schäfer, M., Schirrmacher, R., Bartenstein, P., and Wängler, B. (2011) DOTA derivatives for site-specific biomolecule-modification via click chemistry: Synthesis and comparison of reaction characteristics. *Bioorg. Med. Chem. 19*, 3864−3874.

(67) Moreau, M., Raguin, O., Vrigneaud, J.-M., Collin, B., Bernhard, C., Tizon, X., Boschetti, F., Duchamp, O., Brunotte, F., and Denat, F. (2012) DOTAGA-Trastuzumab. A New Antibody Conjugate Targeting HER2/Neu Antigen for Diagnostic Purposes. *Bioconjugate Chem. 23*, 1181−1188.

(68) Bernhard, C., Moreau, M., Lhenry, D., Goze, C., Boschetti, F., Rousselin, Y., Brunotte, F., and Denat, F. (2012) DOTAGA−Anhydride: A Valuable Building Block for the Preparation of DOTA-Like Chelating Agents. *Chem. - Eur. J. 18*, 7834−7841.

(69) Stasiuk, G. J., and Long, N. J. (2013) The ubiquitous DOTA and its derivatives: the impact of 1,4,7,10-tetraazacyclododecane-1,4,7,10-tetraacetic acid on biomedical imaging. *Chem. Commun. 49*, 2732−2746.